

Article

# Novel Drone Design Using an Optimization Software with 3D Model, Simulation, and Fabrication in Drone Systems Research

Ahmed. O. MohamedZain <sup>1,\*</sup>, Huangshen Chua <sup>2</sup>, Kianmeng Yap <sup>1,\*</sup>, Pavithren Uthayasurian <sup>3</sup> and Teoh Jiehan <sup>3</sup> 

<sup>1</sup> Research Centre for Human-Machine Collaboration, Department of Computing and Information Systems, School of Engineering and Technology, Sunway University, Bandar Sunway, Petaling Jaya 47500, Malaysia

<sup>2</sup> Department of Mechatronics Engineering, School of Engineering, UOW Malaysia KDU Penang University College, Jalan Anson, George Town 10400, Malaysia; hs.chua@kdu.edu.my

<sup>3</sup> School of Electrical and Electronics Engineering, University of Wollongong Malaysia KDU, Glenmarie Campus, Shah Alam 40150, Malaysia; 0128252@kdu-online.com (P.U.); 0122320@kdu-online.com (T.J.)

\* Correspondence: 19102003@imail.sunway.edu.my (A.O.M.); kmyap@sunway.edu.my (K.Y.)

**Abstract:** This paper presents the design of a small size Unmanned Aerial Vehicle (UAV) using the 3DEXPERIENCE software. The process of designing the frame parts involves many methods to ensure the parts can meet the requirements while conforming to safety and industry standards. The design steps start with the selection of materials that can be used for the drone, which are polylactic acid (PLA), acrylonitrile styrene acrylate (ASA), and acrylonitrile butadiene styrene (ABS). The drone frame consists of four main parts, which are the center top cover (50 g), the side top cover (10 g), the middle cover (30 g), and the drone's arm (80 g). A simulation was carried out to determine the stress, displacement, and weight of the drone's parts. Additionally, a trade-off study was conducted to finalize the shapes of the parts and the various inputs based on their priorities. The outcome of this new design can be represented in design concepts, which involve the use of the snap hook function to assemble two body parts together, namely the middle cover and the center top cover, without the need of an additional fastener.

**Keywords:** UAV; polylactic acid; acrylonitrile styrene acrylate; acrylonitrile butadiene styrene; trade-off study



**Citation:** MohamedZain, A.O.; Chua, H.; Yap, K.; Uthayasurian, P.; Jiehan, T. Novel Drone Design Using an Optimization Software with 3D Model, Simulation, and Fabrication in Drone Systems Research. *Drones* **2022**, *6*, 97. <https://doi.org/10.3390/drones6040097>

Academic Editors: Andrzej Łukaszewicz, Wojciech Giernacki, Zbigniew Kulesza, Jaroslaw Pytka and Andriy Holovatyy

Received: 12 February 2022

Accepted: 11 March 2022

Published: 14 April 2022

**Publisher's Note:** MDPI stays neutral with regard to jurisdictional claims in published maps and institutional affiliations.



**Copyright:** © 2022 by the authors. Licensee MDPI, Basel, Switzerland. This article is an open access article distributed under the terms and conditions of the Creative Commons Attribution (CC BY) license (<https://creativecommons.org/licenses/by/4.0/>).

## 1. Introduction

A drone is an aircraft without a human pilot inside and it is also known as an Unmanned Aerial Vehicle. It has many functions and applications such as for medical transport [1], health care service [2], high-rise firefighting [3], drone monitoring application for marine megafauna [4], and many other usages in our current modern society. This research presents a new design concept and creative 3D design idea of a drone that was designed with the 3DEXPERIENCE software. The main reason for using 3DEXperience software for this project is that it is a software that emphasizes having a collaborative environment. Since this project has included a few people, and each with a different role, it has been convenient to use the software for project sharing and discussion all within the platform, especially during the current COVID-19 pandemic situation. The platform itself has a variety of applications within it, which include software for 3D modelling (CATIA and SOLIDWORKS), simulation (SIMULIA), social and collaborative (ENOVIA) as well as information intelligence (NETVIBES) [5]. Therefore, each user can have roles such as project manager, simulation engineer, and 3D designer and use the applications according to their roles. With that, the tasks can be distributed easily based on different roles, the project models and files can be seen and shared by everyone in the group, and the project timeline can be managed within the platform, which allows easy tracking of the project. All these can be done within the same software, which makes the software a good choice for a group project that requires much collaboration. Three dimensional designing through simulation

rather than creating a prototype can reduce the cost for a designer. Since it is a 3D design, engineers can come up with more advanced engineering knowledge and technology. This process is necessary to ensure the parts are able to meet the requirements while conforming to safety and industry standards. While using 3D Modelling, the applications used are Part Design and Assembly Design. This research concentrates on the design phase of the drone. The various designing steps included in this phase are discussed. The objectives of this research are to simulate a drone frame to optimize the bottom cover, to study and compare concept shapes of the top cover, arm, leg bracket, and bottom cover of a drone using a trade-off study, and to analyze the force that is generated by the motors in order to determine how much the drone can handle.

Researchers have a lot of interest in designing the parts of a drone and the design is dependent on the application of the drone, where there are many factors to be considered such as speed-motor selection and airframe selection [6]. In this research project, the design of the drone has been made for parcel delivery purposes, which consists of four DC motors. The single motor has a thrust of 5227 lbs/g. The researchers in [7] studied and analyzed the efficiency of a small quadrotor using air-foils. In this work, the modelling and control design were demonstrated through a series of repeated flights. The researchers in [8] analyzed the aerodynamic interaction between rotors of a micro-quadcopter. Equation (1) was used to calculate the Reynolds number [8], where  $Re$  represents the Reynolds number,  $\rho$  represents the density of air,  $\Omega$  represents the rotor angular velocity, and  $\mu$  represents the dynamic viscosity of air.

$$Re = \frac{\rho \Omega R c}{\mu} \quad (1)$$

Figure 1 depicts the different designs of drone available for development, which are X-design, H-design, and hybrid H-design. Each design has its own advantages and disadvantages. X-design has the advantage of being light and is usually used for racing purposes [9]; however, it requires long landing gear. H-design has the disadvantage of being heavy [10]. Part Design is an integrated application in 3DEXPERIENCE that includes design, weight calculation, and 3D structure. The application's aim is to give a better view of the design when the design is constructed. The Assembly Design application in 3DEXPERIENCE helps to fix the parts that have been designed and shows the constraint between the parts. This can optimize the design and can solve the issue of overlapping. As shown in Table 1, the drone design has a total of six different parts, and they are classified into two main groups. The upper part of the drone is the drone frame and the lower part of the drone is the drone carriage, which is used to carry the payload. The details of the parts included in each of the categories and the number of parts contributing to the overall drone are presented in Table 1. Figure 2 shows the novel design of the drone using 3DEXPERIENCE. Three Dimensional printing, also known as additive manufacturing, is used in this project for the fabrication of the drone frame. With the use of a CAD software, which in this case is 3DEXPERIENCE, the designed models can be sent to a 3D printer and the parts can be printed within a few hours [11–13]. A 3D printer is a device used for computer-aided manufacturing, whereby it creates 3D objects through “printing” and solidifying of materials [11,14], which range from polymers (thermoplastic) to metal and even food [15]. Thermoplastics are the most widely adopted 3D printing material and they come in various forms such as the most used extrusion (also known as filament), resin, and powder [16].

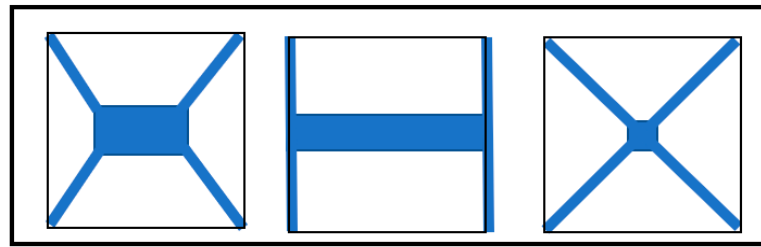


**Figure 1.** Drone hybrid H-design, H-design, and X-design Available for Development [8].

**Table 1.** Drone's Parts.

Category		Part Name	Numbers of Parts
Upper drone	Drone Frame	Centre Top Cover	1
		Side Top Cover	2
		Drone Arm	4
Lower drone	Carriage (Payload)	Middle Cover	1
		Leg Bracket	4
		Bottom Cover	1

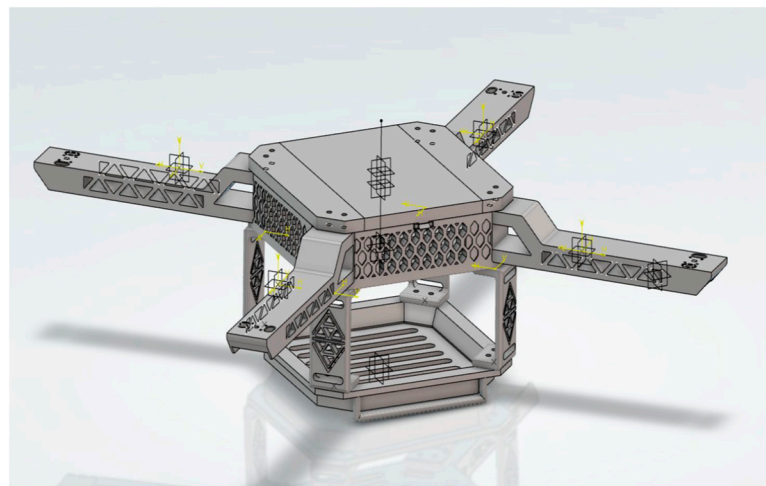


**Figure 2.** Original Design of the Drone using 3DEXPERIENCE.

The technique used for the 3D printing of the thermoplastic is known as the Fused Filament Fabrication (FFF) [17] where the working principle of the desktop FFF 3D printer is originated from the Fused Deposition Modelling technology [18]. The FFF technique works on the principle of fabricating parts layer by layer. The thermoplastic material, which is in the form of a filament roll, is firstly heated and melted then extruded through a nozzle. The nozzle extrudes the melted filament to a platform in layers based on the predefined pattern of the model [19,20]. The figure below shows an example of a desktop FFF 3D printer.

Using the technology of 3D printing, a wide range of applications can be performed, which range from manufacturing UAV parts with different functionalities and specifications [21–24] to fabricating medical devices [25], and even the field of musical instrument research [26]. This shows that 3D printing has a high potential in diverse applications.

## 2. Materials and Methods

In this section, a simulation model of the drone is presented by using 3DExperience software, where an overview of the drone frame and the originality of the design is provided. The type of chassis of the frame used in this design is X-Chassis. Choosing this chassis rather than the (+) chassis or H chassis ensures that the drone can be stable. This chassis can

hover longer compared to other chassis and it is easy to control and maneuver. The suitable location for the center of gravity is in the middle of the drone, which will make controlling the drone easier and will make the drone more stable. Therefore, the components' weight will be distributed on the drone based on the most suitable position for the center of gravity. The momentum theory represents the basic understanding of the drone motion, where the thrust is calculated based on this theory [26].

The general forces considered for all parts are the gravity, the landing force, and the lifting force as shown in Table 2. The gravity will usually be at the center of the part with a standard value of 9.8 m/s or 9.8 N/kg. These slight forces may have an effect; thus, they have been included in the consideration for the design of the parts. In normal conditions, when the drone lands, the force acting on it is the weight of the whole drone with the payload or without the payload if it is a return journey. Thus, the landing force can also be considered as the weight of the drone. On the other hand, the lifting force occurs when the motors turn the propellers and lift the drone. Each of the motors will produce a lifting force of 5 N, hence, giving a total lifting force of 20 N. Equation (2) [27] represents the thrust in terms of mathematical samples, where  $T$  is the thrust measured in Newton (N),  $A$  is the area of the propeller rotor in meter square ( $m^2$ ),  $\rho$  is the density of the air in kilogram per cubic meter ( $kg/m^3$ ),  $v$  is the velocity of the air at the propeller in meter per second ( $m/s$ ), and  $\Delta v$  is the velocity of the air accelerated by the propeller in meter per second.

$$T = A \times \rho \times v \times \Delta v \quad (2)$$

**Table 2.** Landing and Lifting Forces.

<b>Landing Force</b>	
1 part	1600 g/15.6906 N
2 parts	800 g/7.8453 N
4 parts	400 g/3.9227 N
<b>Lifting Force</b>	
1 part	20 N
2 parts	10 N
4 parts	5 N

### 2.1. Drone Frame and Originality in Design

The drone frame consists of parts that will be used to place the controller, the battery, the motor, etc. Figure 3 illustrates the design of the drone arm, center top cover, side cover, and middle cover. The outcome of this new design can be represented in design concepts through the use of the snap hook function to assemble 2 body parts together, namely the middle cover and the center top cover, without the need of an additional fastener. Figure 3c shows the cantilever snap fit design. This design will help to reduce extra cost and the weight of the drone. It will also reduce the time needed when performing maintenance. Furthermore, snap fit allows the process of assembly and disassembly of the parts to be carried out easily. The body of the drone was designed referring to honeycomb design. Honeycomb sandwich structures are frequently used to attain these aims in the aerospace, automotive, housing, packaging, and sports equipment sectors, among others [28]. A honeycomb construction is created by sandwiching an array of hollow tubes or cells between two solid walls. The advantage of the design is also reducing weight and it increases the structure impact resistance. It also increases the cooling of the electrical components and increases the lifespan of the components. The honeycomb design can carry weight as well as being a light structure. The hexagonal shape of the honeycomb design is usually the strongest shape. This design will be more rigid and also lightweight, where it is a new concept in drone designs. Other than that, it also increases the air flow in the middle cover where the components are placed. This can cool down the electronic components and can reduce overheating.

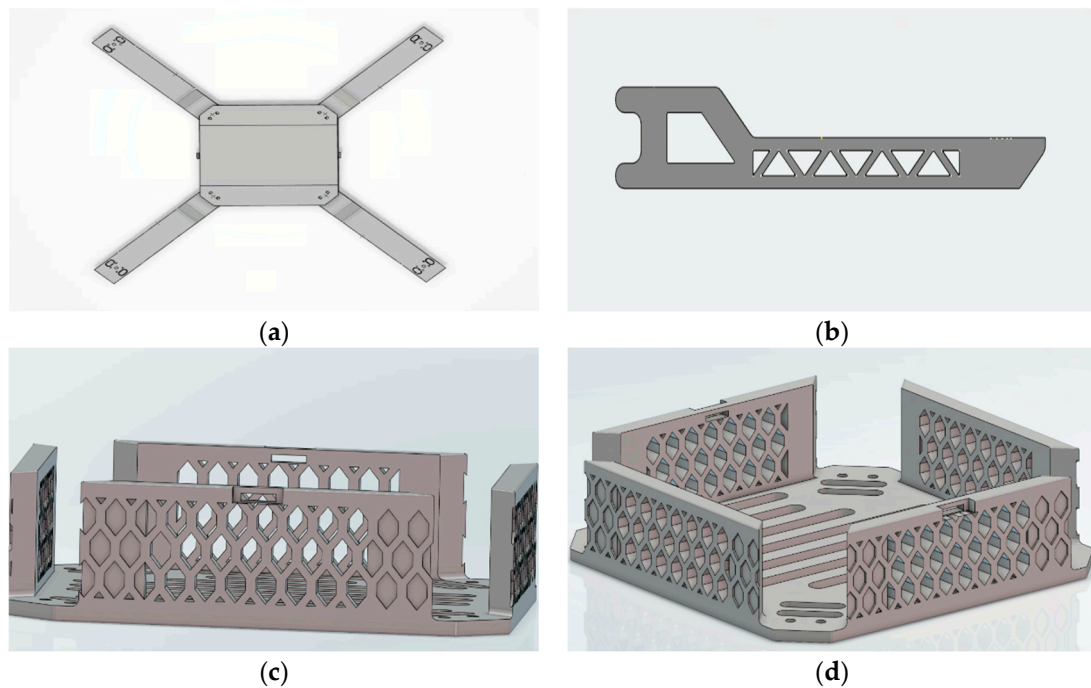


**Figure 3.** Drone's Frame Design. (a) Top View of Drone. (b) Drone's Arm. (c) Cantilever Snap Fit Design for Side Cover. (d) Cantilever Snap Fit Design for Middle Cover.

## 2.2. Material Selection

The focus of the project is to design a lightweight quadcopter drone for parcel delivery purposes. From the material specifications, both ASA and ABS have a similar density value. However, ABS material has a higher Young's Modulus, which indicates that the material is stiffer as compared to ASA [29]. On top of that, the maximum stress that ABS can take before breaking is also higher than ASA, which makes it good for parts such as the drone arm that requires some flexibility since it is attached to the motors that will provide lifting force.

Although the weather and thermal resistant properties of ASA are higher than ABS [30,31], there are a few drawbacks of using ASA. ASA is more expensive, and it has a lower market availability as compared to ABS [32]. On top of that, ASA can be difficult to print as it requires a higher extruder temperature during the printing process; hence, it is harder to facilitate. Since the electronics components used will not produce too much heat, ABS is chosen to be used as it can fulfil the requirements and budget constraints. According to [33], the glass transition temperature ( $T_g$ ) of PLA is between 55 °C and 80 °C depending on the different types of molecular weight and stereochemistry, while the melting point ranges between 130 °C and 180 °C. Thus, these temperature ranges should be sufficient for the average temperature in Malaysia, which falls within 21 °C and 32 °C [34]. The materials used for the drone are PLA, ASA, and ABS. The materials were defined in 3DEXPERIENCE using the Material Definition App according to the values given in Table 3. However, PLA and ABS material are chosen to be used in the final design of the drone. PLA is used for most parts that need to be denser, stiffer, and stronger, as it can protect the inner part of the drone, while ABS material is chosen to be used for some parts to reduce the overall weight of the drone since it is light but is still much stiffer and can withstand a greater stress before breaking as compared to ASA material. Only the core material is defined because the covering material does not have much effect during the simulation. Figures 4–6 show the materials chosen to be used from 3DEXPERIENCE and their stress–strain curves, which show the maximum stress that can be withstood before breaking. On top of that, the maximum stress suggested that the deflection of a part should

be less than 4.7 mm, as shown in the setting of the materials using the Material Definition App and their respective stress–strain curves.

**Table 3.** Material Specifications.

Material	PLA	ASA	ABS	PETG
Density (kg/m <sup>3</sup> )	1240	1070	1050	1270
Young’s Modulus (MPa)	$1.98 \times 10^9$	$1.35 \times 10^9$	$1.70 \times 10^9$	$1.38 \times 10^9$
Poisson Ratio			0.33	
Maximum Stress before breaking (MPa)	47	28	35	-

The drone is to be manufactured using 3D printing. In general, there are 4 types of material that can be used while performing FDM/FFF Thermoplastics 3D printing and they are PLA, ASA, ABS, and PETG. Each of them provides a different performance based on the nature of the material. Since the objective of this project is to build a drone that is lightweight but strong enough to fly at a certain height for the longest period of time, the main characteristics that need to be assessed are the density and the Young’s Modulus of the materials.

For the center top cover, the material selected to be used as the core material is ABS material. Since this part implements the snap hook system, it has to be slightly flexible; moreover, ABS material is not too stiff as compared to PLA material. For the side top cover and the middle cover, the material selected to be used is PLA material. This is because PLA is stiffer and stronger than the other materials as mentioned earlier. Thus, it can “protect” the inner accessories of the drone as the battery, controller, ESC, etc., that are utilized for controlling the drone will be inside these parts. For the drone arm, the material selected to be used as the core material is ABS material. This is because ABS is stiffer as compared to ASA material, but it is lighter as compared to PLA material. Thus, it can bend slightly without breaking since it is not too stiff, as the drone arm will be directly connected to the motor.

### 2.3. Sketch Constraint and Design for Manufacturability

Constraints are ideal for creating practical 3D printing objects. It is important to pick the sketch objects that are desired to be limited in order to apply a constraint and click the corresponding constraint in the menu. The order in which the objects are picked will also influence how the constraint is implemented. The costs of manufacturing a drone can be reduced by designing a part or assembly for manufacturability. Manufacturability refers to the situation where a product can be quickly assembled from fewer parts. For example, the whole drone design is made up of six parts, which are shown in Table 1. Thus, this product is easier to be assembled and built in a shorter period of time. The parts of the drone are designed with standard sizes and they are easier to fabricate. This helps to optimize the parts of the drone such that it can be created more easily and at a cheaper cost. Reducing the cost and increasing the quality will make sure the product is sustainable in the market. The labor cost is also reduced, thanks to the fewer parts.

### 2.4. Carriage (Payload) and DOF

The most important factor when flying a drone is the degree of freedom (DOF). This factor has a large impact when it comes to the stability of the drone in maneuvering and travelling over a distance. The six main parts’ DOFs should be followed to ensure more smooth and stable movements. Referring to the drone designed, it can move longitudinally, vertically, and laterally. This will also ensure the drone can make roll, pitch, and yaw movements on each axis.

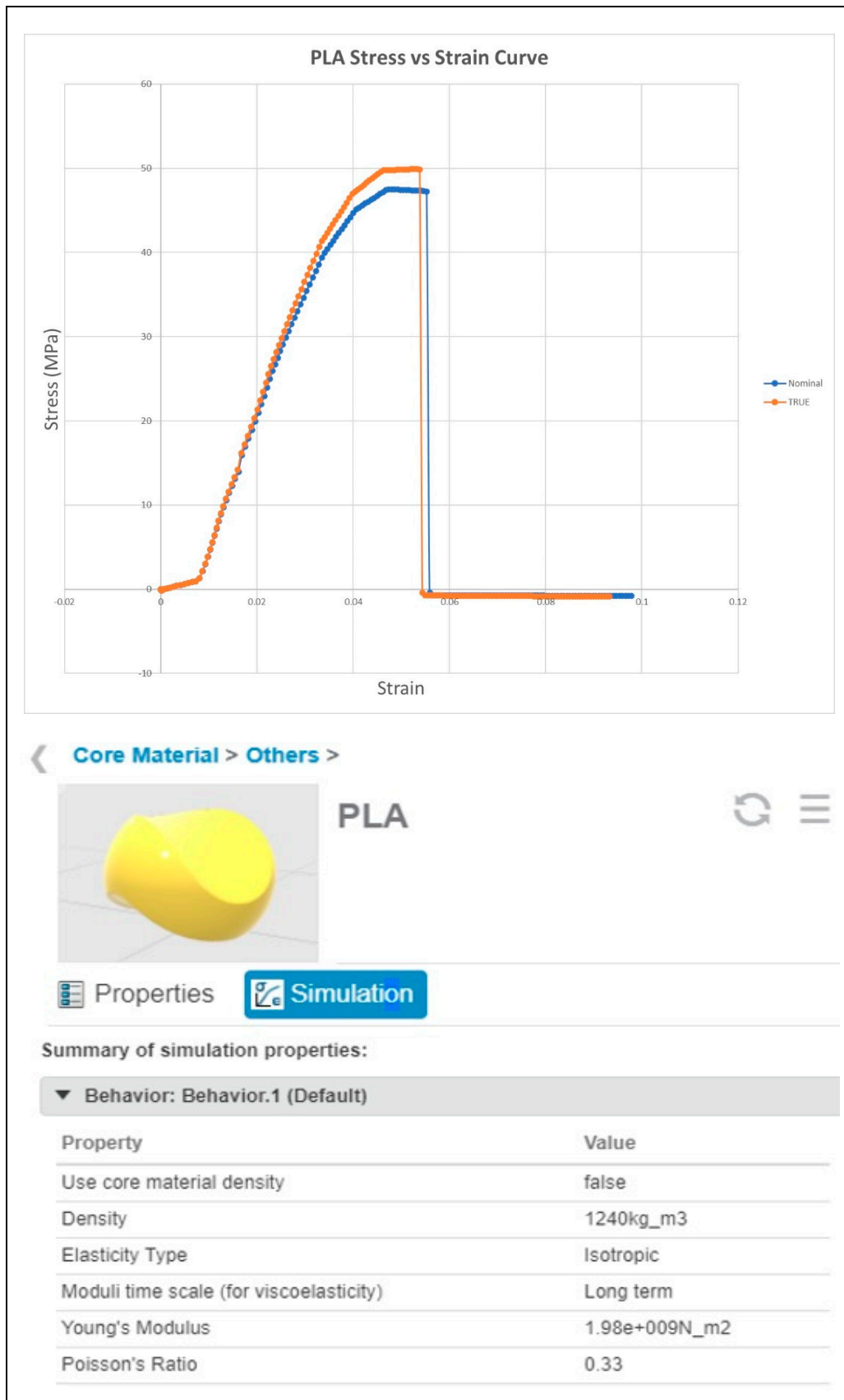


Figure 4. PLA Stress Curve.

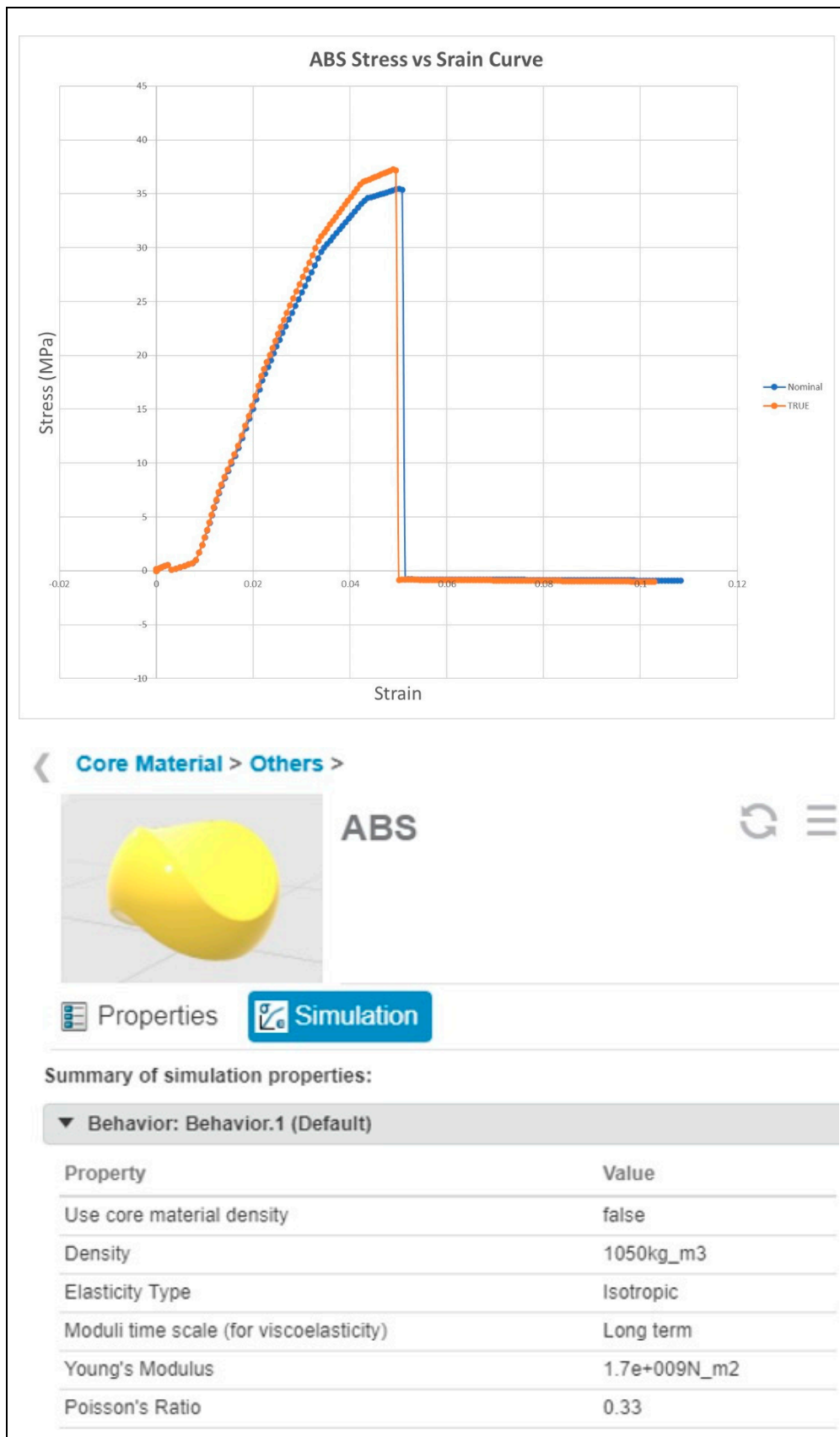


Figure 5. ABS Stress Curve.



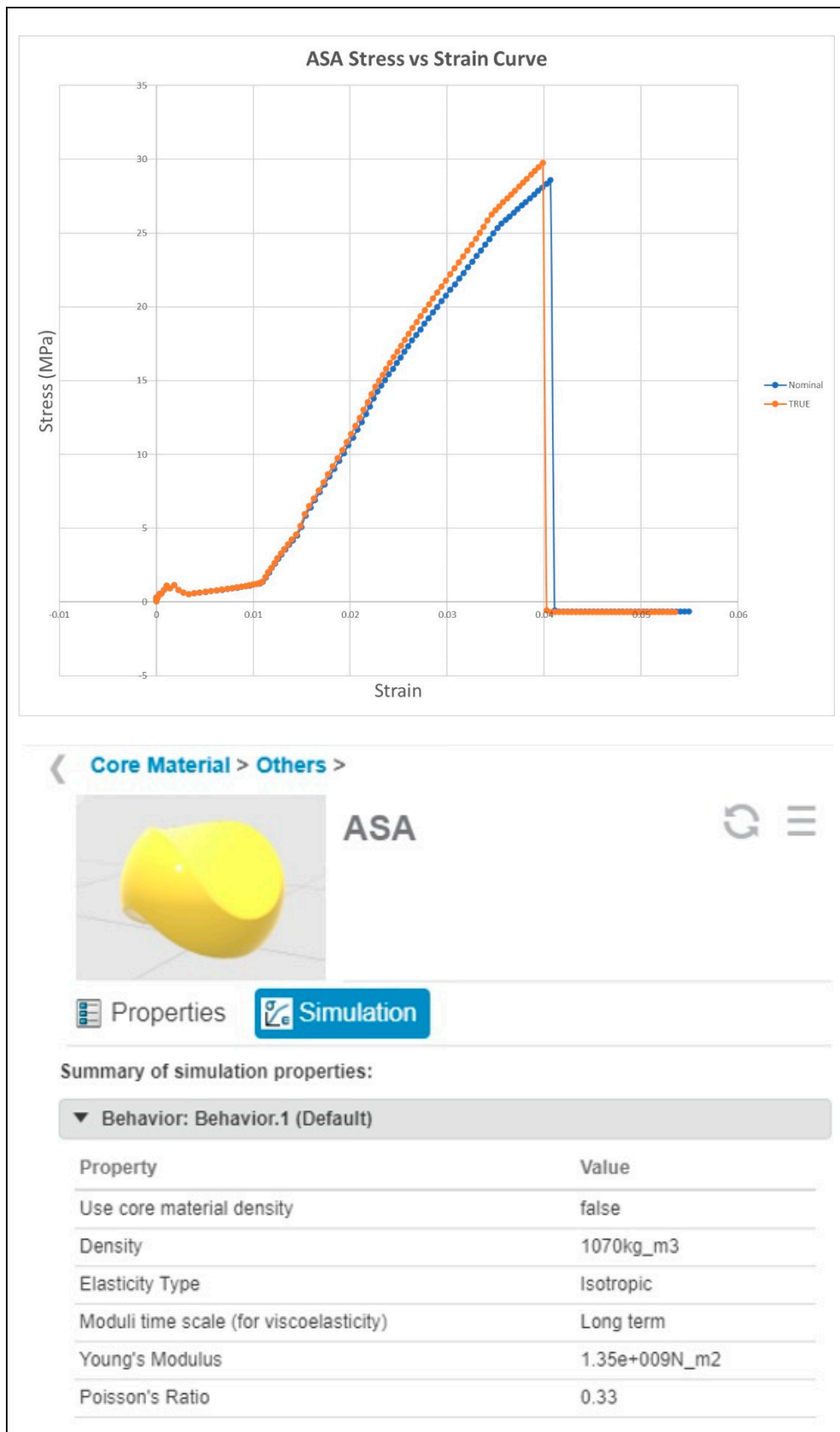





Figure 6. ASA Stress Curve.

### 3. System Simulation

Due to their wide range of applications, the attention towards drones has been constantly growing for the past decade. With the help of CAD software, many studies have been conducted to continue optimizing the performances of current drones in recent years while adapting the use of 3D printing technologies because they will play an integral part in the fourth industrial revolution [35]. Table 4 represents several examples of drone designs. Three Dimensional printing, which is a type of rapid prototyping, allows the low cost of drone fabrication [36,37], while CAD software enable the simulation such as the finite element analysis (FEA) to be carried out [38]. The main application used to simulate the design of the drone is the Functional Generative Design (FGD) application. Generative design is a revolutionizing product design and development technique of exploring multiple permutations of a solution to obtain the best design option. This application aims to optimize manufacturability and create a lightweight design; hence, saving material usage during manufacturing of the product. By applying different inputs based on the requirement and target, multiple variations can be generated in the system, which allows the user to perform a trade-off study to compare and analyze the options available. Finally, a detailed design can be constructed based on the chosen design for additive manufacturing.

**Table 4.** Several examples of drone designs.

Drone Type	Designs of Drones	Material Used
PoliDrone UAV [36]		Customizable multirotor drone frame
Iris + drone [39]		Drone frame can be printed using the Fused Filament Fabrication (FFF)
Skeleton X-14 Quadcopter [40]		FFF-printable with a single-piece body

As well as the FGD application, another element that is used is the Linear Structural Validation (LSV) application. This application is used to provide a simple insight into the design; hence, informed design decisions can be made easily. It is based on a powerful finite element solver that allows complex simulations. The four types of methods available for LSV are static stress, buckling, frequency, and thermal. This is usually used at the end of the design process to validate the final model used. Static stress analysis is used in this project, which includes evaluation of the stress, strain, and displacement of the model.

### Restrain/Connection

For the center top cover, restraining is performed using a “clamp” at both inner sides of the part as shown in Figure 7a. The two sides will be attached to the middle cover using a snap hook system; therefore, it should be fixed throughout the flight. For the side top cover, restraining is performed using a “clamp” where the four holes at the sides are clamped as shown in Figure 7b. The four holes will be bolted to the middle cover; hence, the degree of freedom should be fixed as it is undesired for the part to move. For the middle cover, restraining is performed using a “clamp” at the eight holes, which are at each of the corners as well as at the side of the middle part that will be connected to the top cover using the snap hook system as shown in Figure 7c. The eight holes will be bolted to the leg bracket and the drone arm as well as the side top cover; thus, the degree of freedom should be fixed as it is undesired for the part to move. As well as that, the sides where the snap hook system is applied are clamped as well because they will be connected to the center top cover.

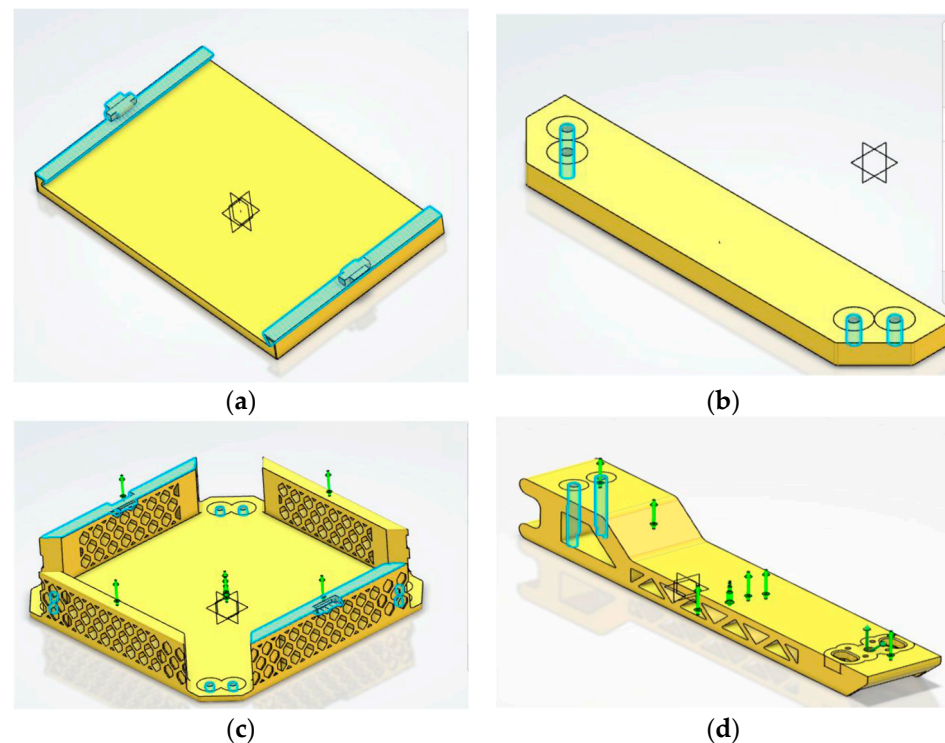


**Figure 7.** Restraining of the Drone Parts. (a) Center Top Cover. (b) Side Top Cover. (c) Middle Cover. (d) Arm.

For the drone arm, restraining is performed using a “clamp” at the two holes at the end of the part as shown in Figure 7d. The two holes will be bolted in between the side top cover and the middle cover; therefore, the degree of freedom should be fixed because the part should not be moving.

## 4. Results and Discussion

### 4.1. Drone's Parts' Stress and Displacement

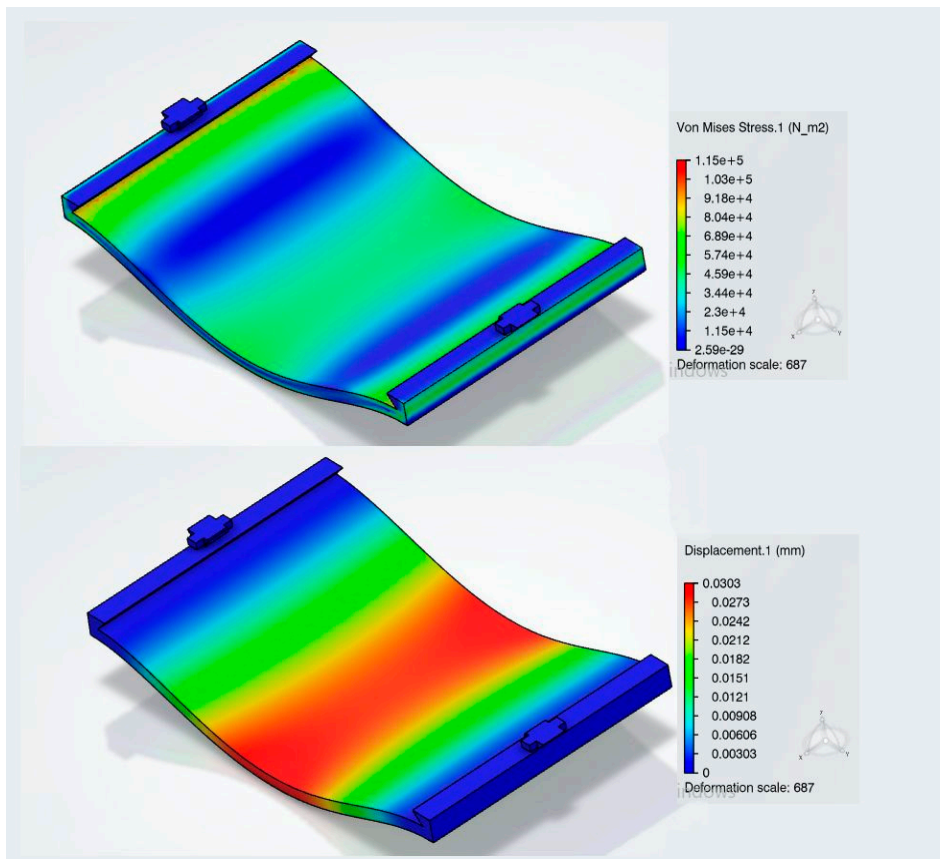
Figure 8 shows the simulation results of the drone frame, which includes the center top cover, the middle cover, the side top cover, and the drone arm. From the results obtained, it is safe to conclude that the drone frame will not fail when it needs to sustain the maximum possible lift force from the motor as well as during the landing process. This is because the Setup Validation showed that the stress and the displacement of the parts were within the accepted range. Furthermore, for the parts that looked bent after going through the simulation, the values were actually very small and insignificant. Figure 9 illustrates the

simulation results of the drone carriage that is used to carry the payload, and it includes the leg bracket and the bottom cover. Similar to the rest of the parts in the drone frame, the deformation value was actually very small. For future enhancements, a slight optimization of the center top cover and side top cover can be performed because the parts have a very plain surface, where some unnecessary edges can be removed to reduce the weight of the parts. However, the optimization conducted will just be minimal because these parts will be used to cover up the components inside the drone; hence, it should not have too many holes or else the components may drop out during the flight. Similar to the center top cover and the side top cover, the middle cover can also be optimized, but not by much since this is the part where the components will be placed and it is undesired for the parts to drop off during the flight. As for the drone arm, the part is still very bulky even though a more optimized design is used to start off with. Hence, the optimization process can also be performed for this part to reduce its unnecessary weight.

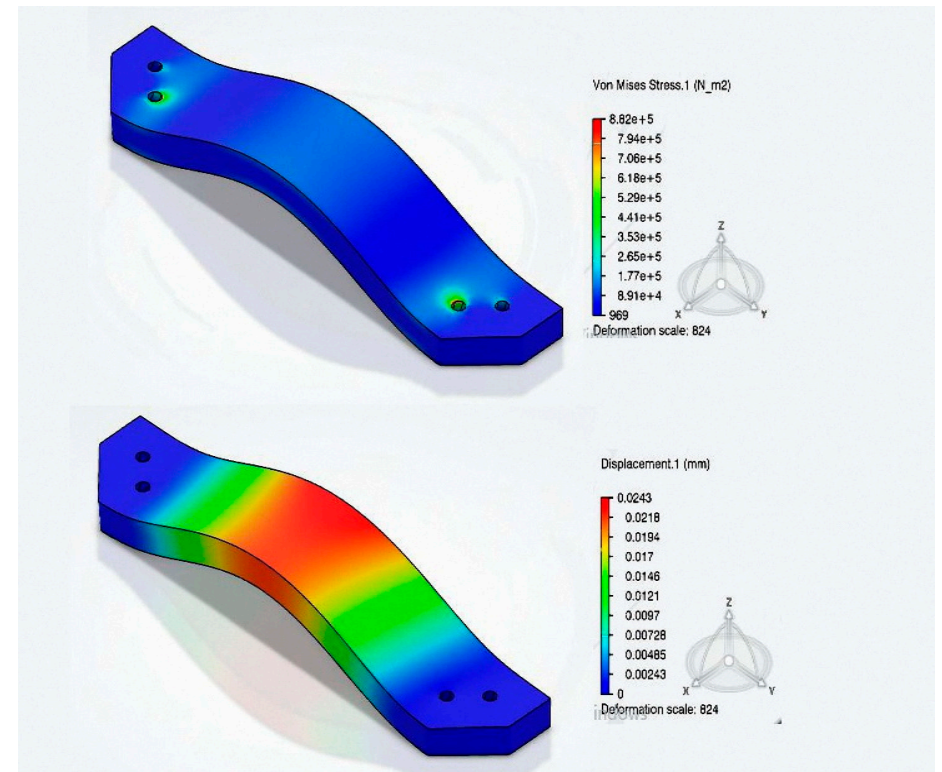
#### *4.2. Trade-Off Study*

For the center top cover, the top four concept shapes generated were compared by performing a trade-off study. The variants that were assessed were the mass, the displacement, and the stress of the part. The mass was given the highest priority; hence, it was set to have a key performance indicator (KPI) of 5. The target of the mass was also set. As well as that, the stress and displacement were given a KPI of 3 as they were less important for this part as it is connected at both ends. As shown in Figure 10, based on the variants and their respective KPIs, the first design scored the highest with a score of 60.3502. However, since this part is supposed to cover up the components inside, it is not suitable for it to have a big hole at the middle of the part. Thus, Centre Top Cover Sim 1 Shape Validation 5, which scored the second highest, was chosen to be the final design since the other variants were still in the acceptable range. For the side top cover, only two concept shapes generated were compared by performing a trade-off study since not much optimization can be conducted for this part.

The variants assessed were the mass, the displacement, and the stress of the part. The mass was given the highest priority; hence, it was set to have a KPI of 5. As well as that, the stress and displacement were given a KPI of 3 as they were not that important for this part as it is connected at both ends. As shown in Figure 11, based on the variants and their respective KPIs, the first design scored higher as compared to the second design with a score of 100. Thus, Side Top Cover Sim 1 Shape Validation 2 was chosen to be the final design since the other variants were still in the acceptable range. For the middle cover, the top three concept shapes generated were compared by performing a trade-off study. Similarly, the variants assessed were the mass, the displacement, and the stress of the part. The mass was given the highest priority; hence, it was set to have a KPI of 5. As well as that, the stress and displacement were given a KPI of 3 as they were not that important for this part as it is connected at all corners.

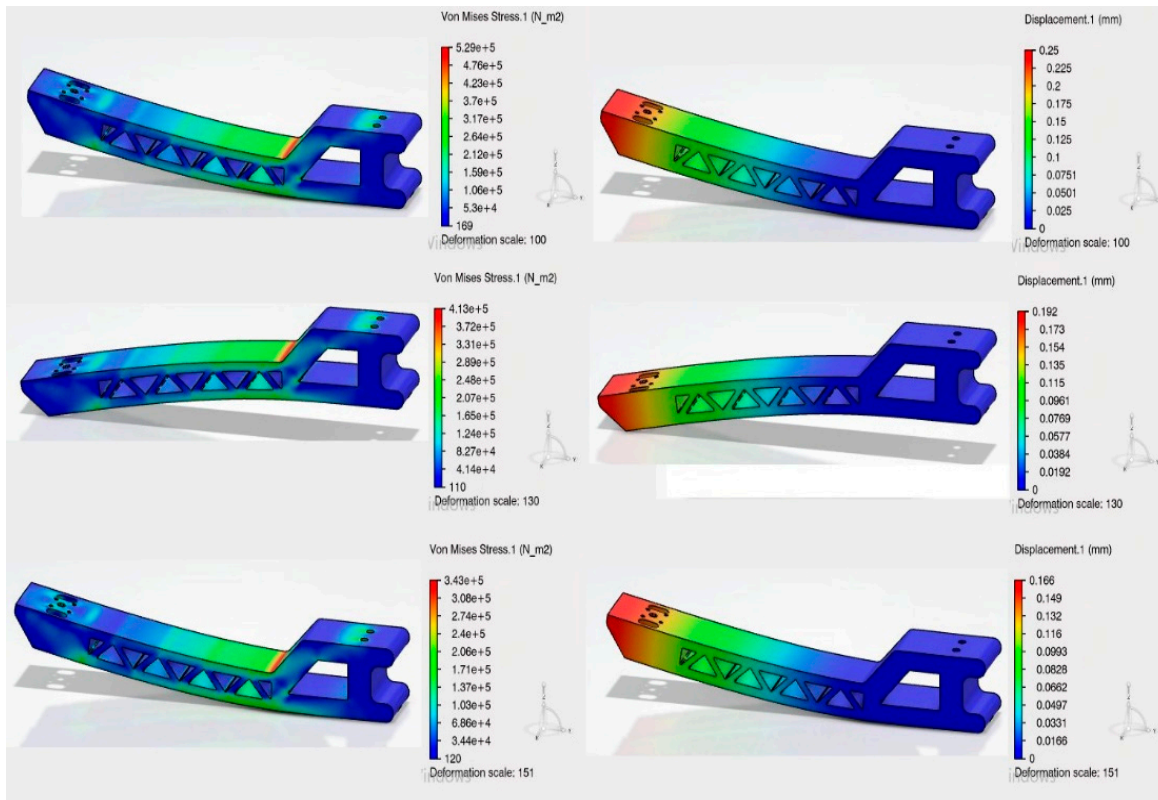


(a)

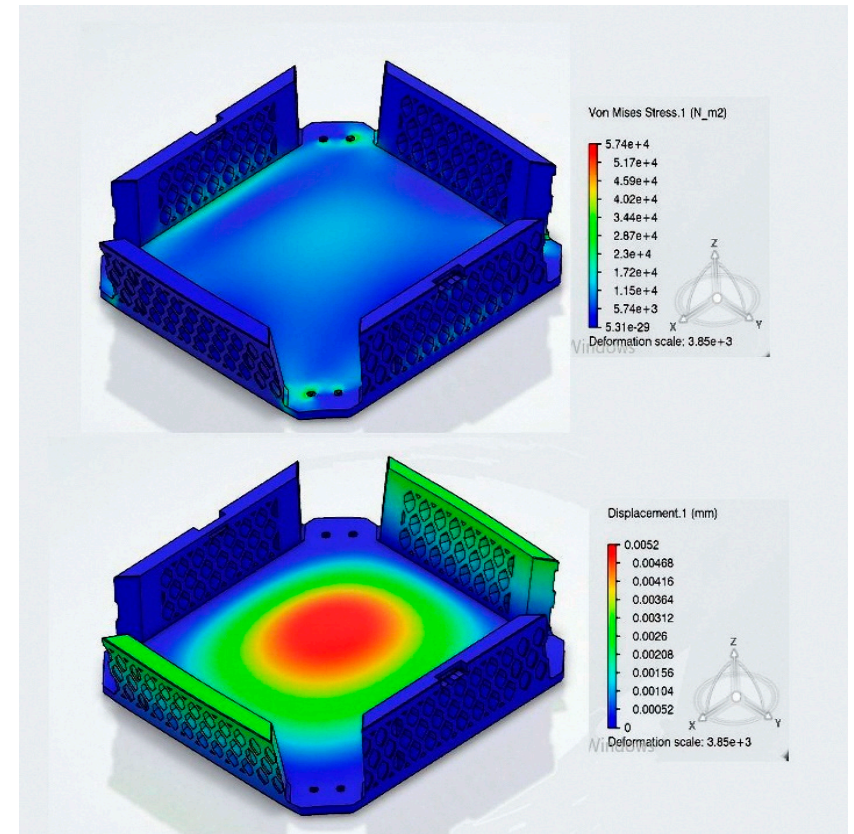


(b)

Figure 8. Cont.

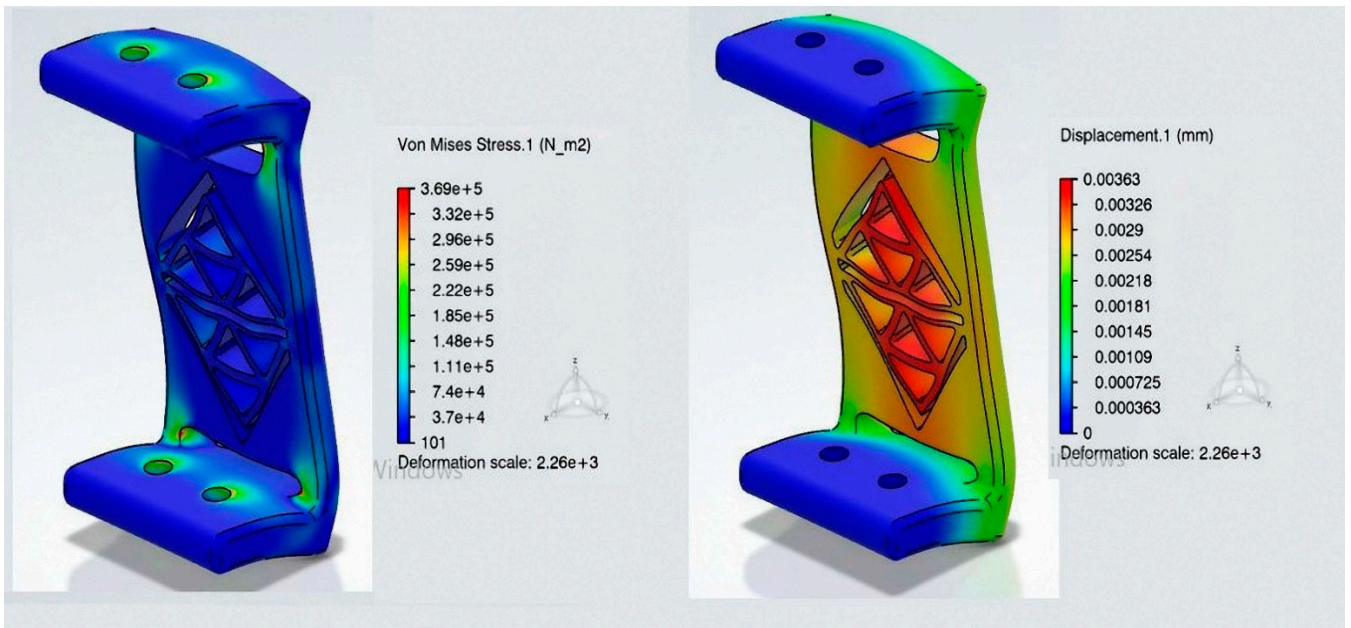


(c)

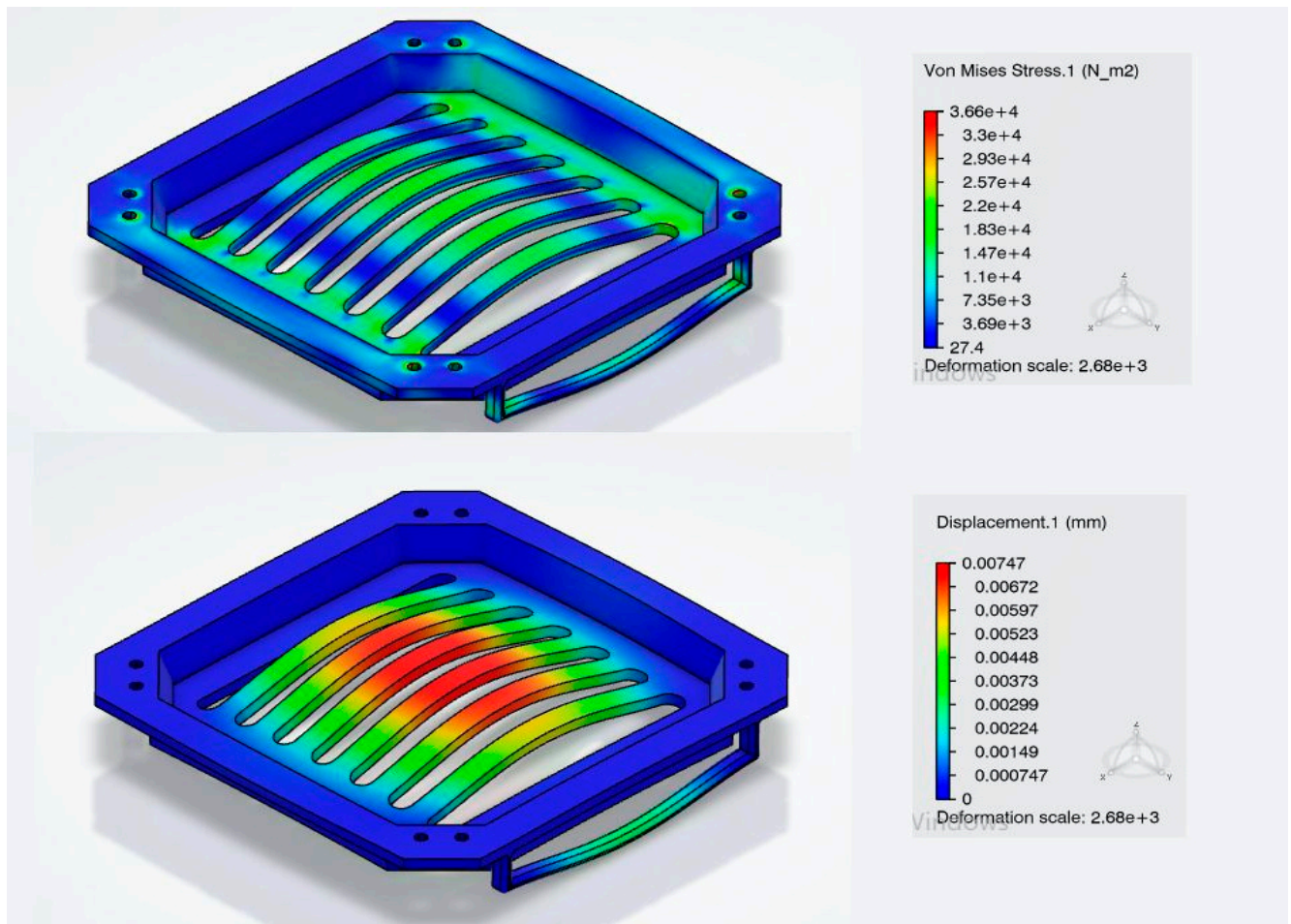


(d)

Figure 8. Stress and Displacement of the Drone's Parts. (a) Centre Top Cover. (b) Side Top Cover. (c) Drone's Arm. (d) Middle Cover.



(a)



(b)

Figure 9. Drone's Carriage Stress and Displacement. (a) Leg Bereket. (b) Bottom Cover.

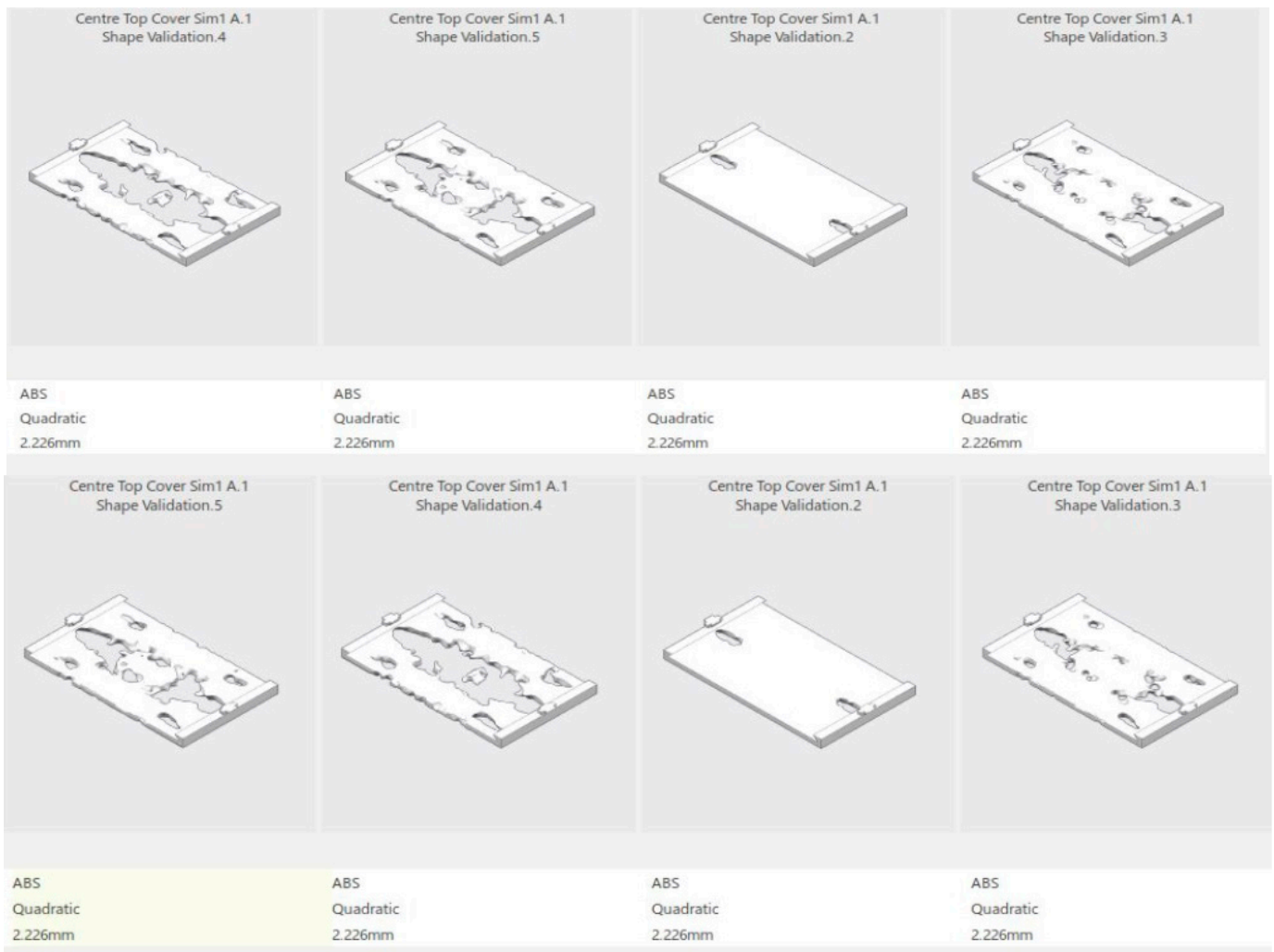


Figure 10. KPI of Centre Top Cover.

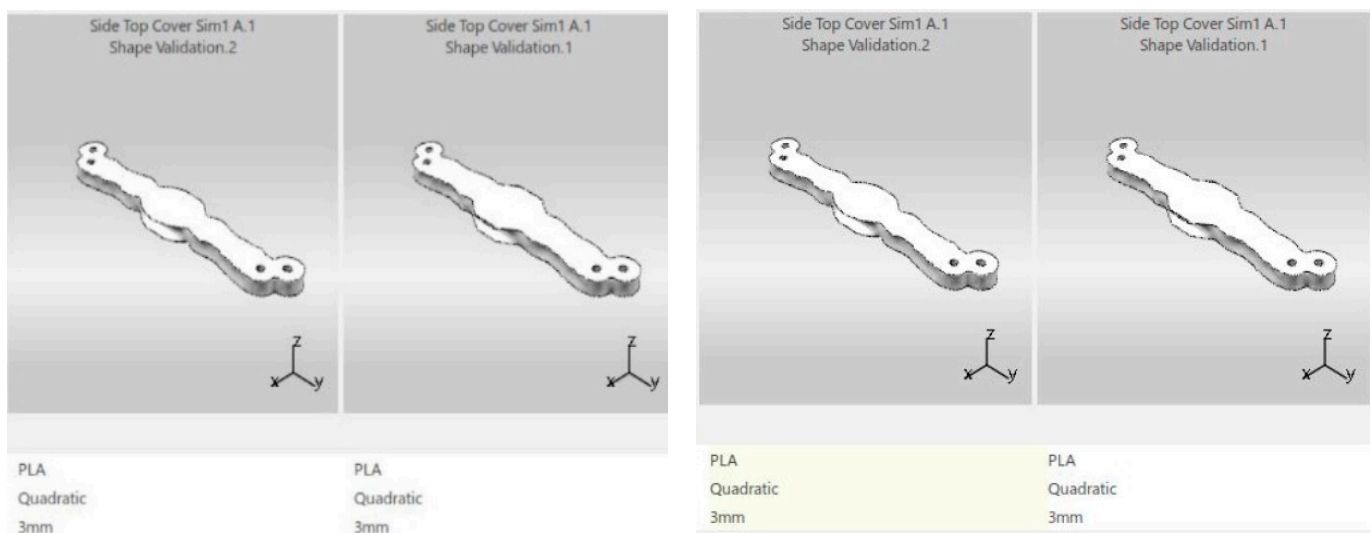


Figure 11. KPI of Side Top Cover.



As shown in Figure 12, based on the variants and their respective KPIs, the first design scored the highest with a score of 87.8811. Thus, Middle Cover Sim 2 Shape Validation 2 was chosen to be the final design as all the other variants were in the acceptable range as well. A trade-off study was conducted for the drone arm, where the top four concept shapes generated were compared. The variants assessed were the mass, the displacement, and the stress of the part. The mass was given the highest priority; hence, it was set to have a KPI of 5. As well as that, the stress and displacement were given a KPI of 4 as they were slightly more important as compared to the previous parts because one end of this part is not be clamped to the other parts. As shown in Figure 13, based on the variants and their respective KPIs, the fourth design scored the highest with a score of 90.2502. Thus, Drone Arm Sim 2 Shape Validation 6 was chosen to be the final design as all the other variants of the parts were in the acceptable range as well. For the leg bracket, the top three concept shapes generated were compared by performing a trade-off study. The variants assessed shapes the mass, the displacement, and the stress of the part. The mass was given the highest priority; hence, it was set to have a KPI of 5. The targeted mass was also inserted. On the other hand, the stress and displacement were given a KPI of 3 as they were not that important for this part since it is connected to both the top and bottom. As shown in Figure 14, based on the variants and their respective KPIs, the third design scored the highest with a score of 54.5. However, the mass of that part differed quite a lot from the targeted mass. Hence, Leg Bracket Sim 3 Shape Validation 2 that scored slightly lower but had a mass that was closer to the targeted mass was chosen to be the final design since the other variants were still in the acceptable range. For the bottom cover, the top three concept shapes generated were compared by performing a trade-off study. The variants assessed were the mass, the displacement, and the stress of the part. The mass was given the highest priority; hence, it was set to have a KPI of 5. The targeted mass was also inserted. On the other hand, the stress and displacement were given a KPI of 4 since they were equally important after the mass.

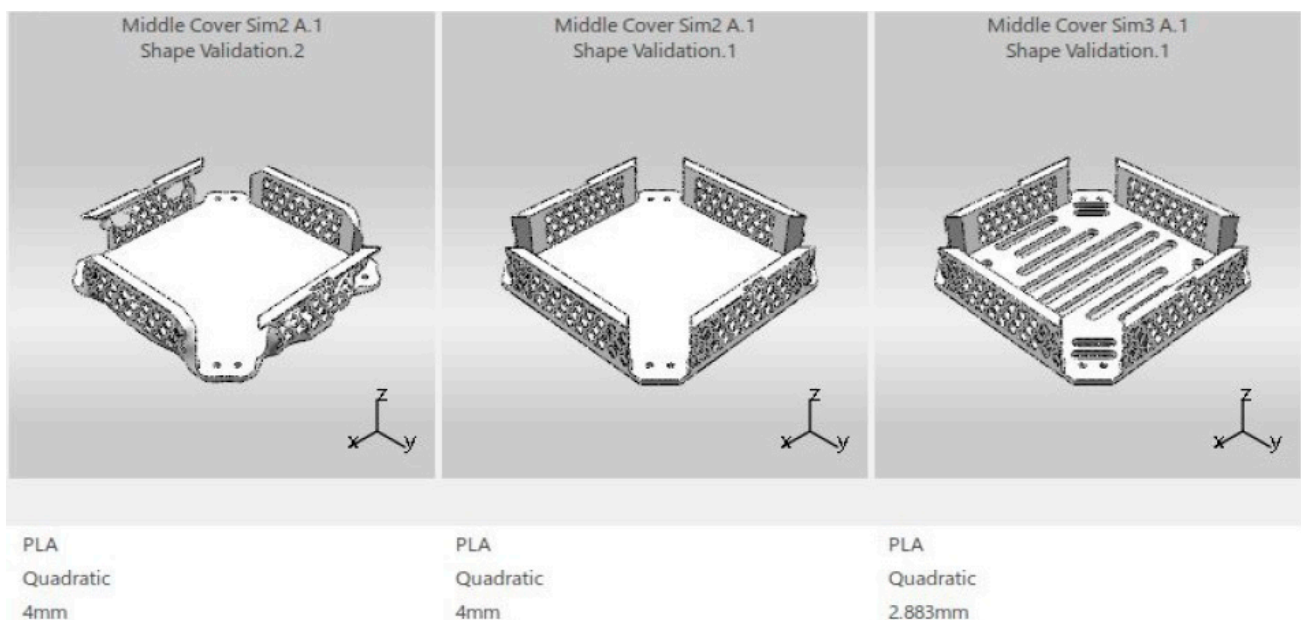


Figure 12. Cont.

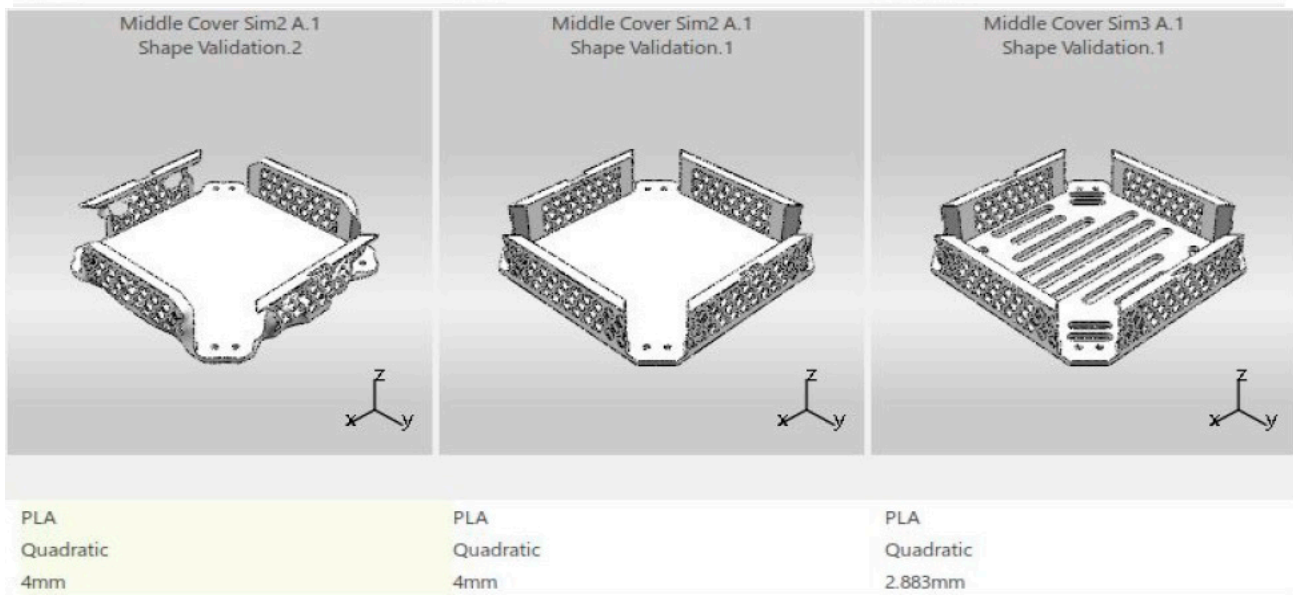


Figure 12. KPI of Middle Cover.

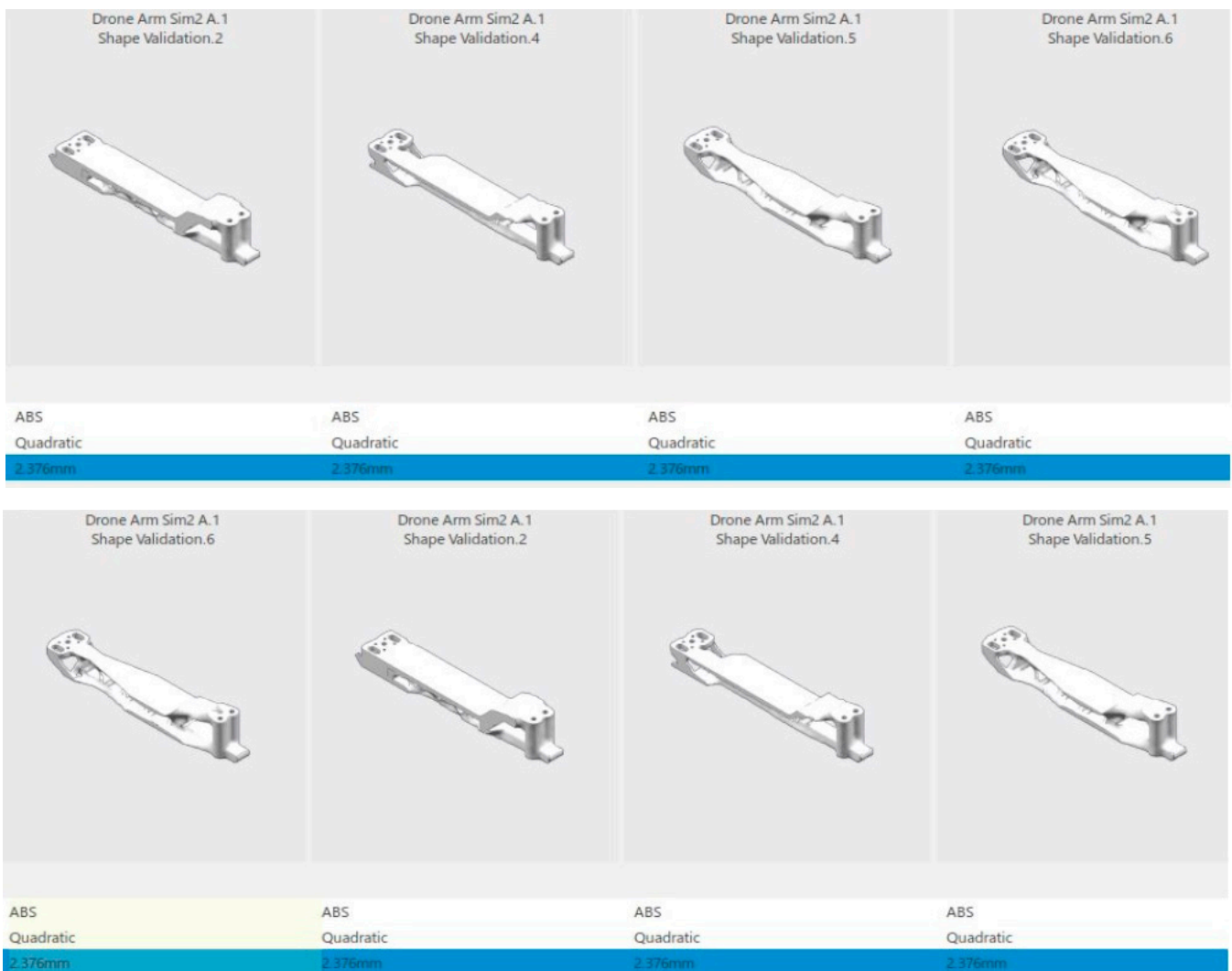
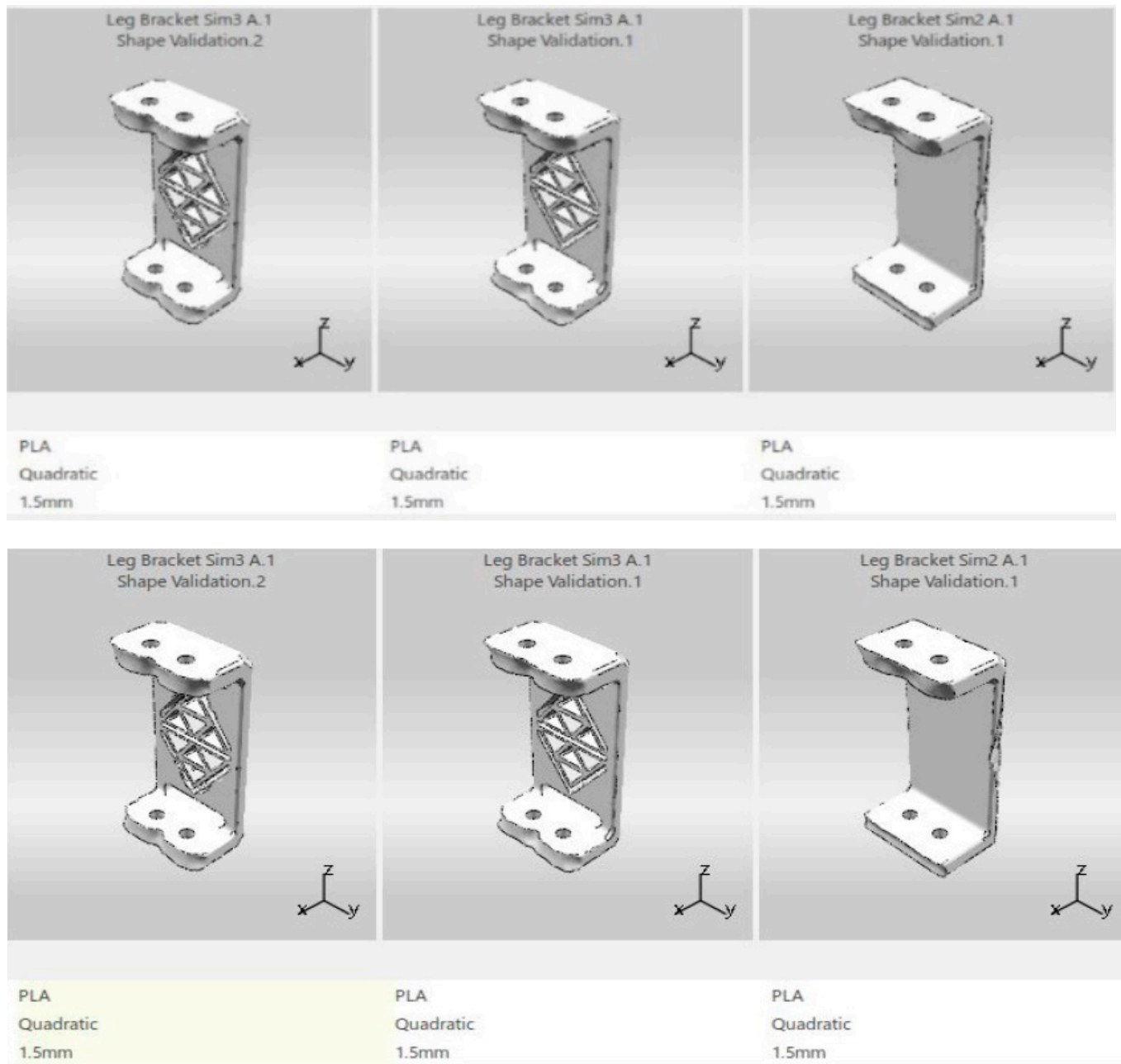
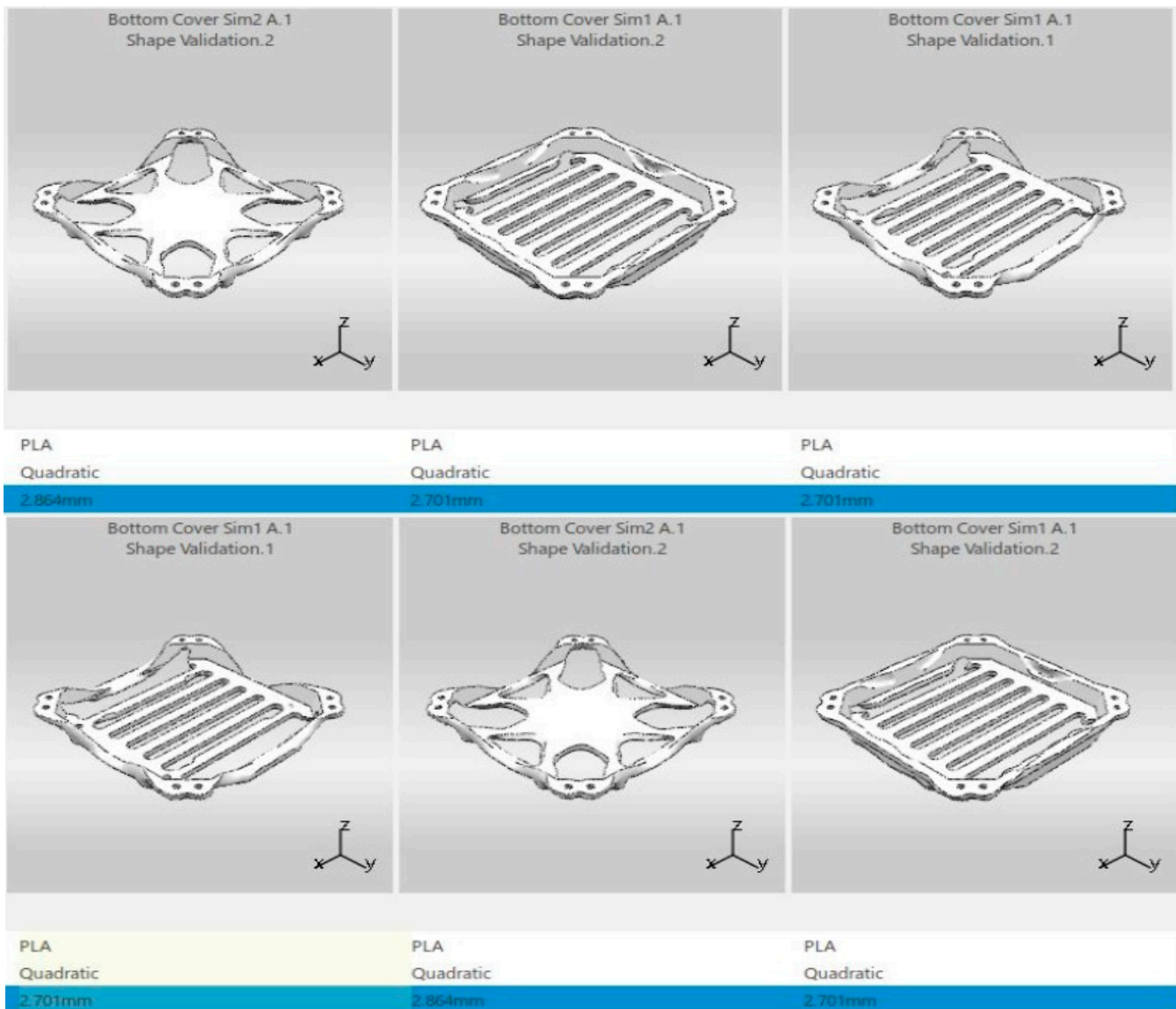


Figure 13. KPI of Arm.



**Figure 14.** KPI of Leg Bracket.

As shown in Figure 15, based on the variants and their respective KPIs, the third design scored the highest with a score of 84.4588. The stress and the displacement were within the acceptable range as well. Furthermore, it was not the lightest design, the stress was lower as compared to the first design, and it had the smallest displacement. Therefore, Bottom Cover Sim 1 Shape Validation 1 scored the highest among the three designs and it was chosen to be used as the final design.



**Figure 15.** KPI of Bottom Cover.

#### 4.3. Simulation Results of Drone's Weight

The Centre top cover was set to have a weight of 0.050 kg as shown in Figure 16a. It was set based on the initial assumption, where this part's targeted weight was at 50 g. The simulation was set to run for 150 cycles to produce the maximum stiffness for a given mass and it was shown that the target weight was reached at the end of the simulation. The side top cover was set to have a weight of 0.015 kg as shown in Figure 16b. This is based on the initial assumed weight, where this part's targeted weight was at 15 g each. The simulation was set to run for 50 cycles to produce the maximum stiffness for a given mass, where the simulation results show that the weight was suitable for this part and the target weight was reached at the end of the simulation. The execution stopped at the 46th cycle when all the constraints had been met. The middle cover was set to have a weight of 0.1 kg as shown in Figure 16c. The value of the weight was determined based on the initial assumed weight, where this part's targeted weight was at 100 g. The simulation was set to run for 80 cycles to produce the maximum stiffness for a given mass, where the simulation results show that the weight was suitable for this part and the target weight was reached at the end of the simulation. The execution stopped at the 68th cycle when all the constraints had been met. The drone arm was set to have a mass of 0.8 kg as shown in Figure 16d. Although the

initial assumed weight showed that the targeted mass of this part was 30 g, the preserved faces already had a mass of 30 g. Therefore, the system would have to remove everything to reach the target, which is not possible. With that, the target mass was increased slightly to 80 g. The simulation was set to run for 80 cycles to produce the maximum stiffness for a given mass, where the simulation results show that the weight was suitable for this part and the target weight was reached at the end of the simulation. The execution stopped at the 76th cycle when all the constraints had been met.

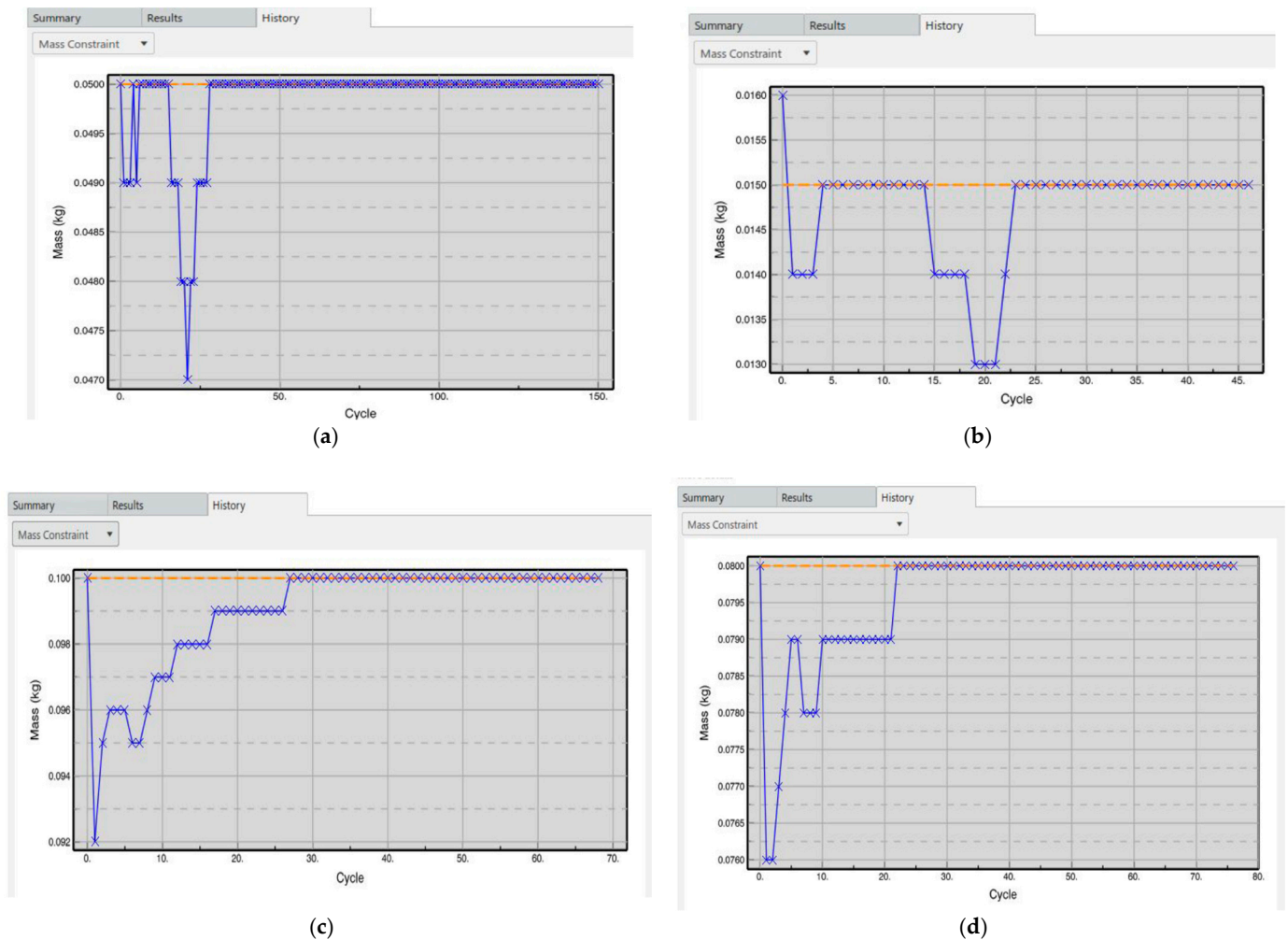


**Figure 16.** Output Weight of the Drone's Parts. (a) Center Top Cover. (b) Side Top Cover. (c) Middle Cover. (d) Drone's Arm.

#### 4.4. Final Hardware Design

As shown in Figure 17, the final design of the drone consists of four main parts referred to in the Supplementary Material. The first part is the middle cover, which has the advantages of being lightweight and having good heat dissipation. The second part is the top cover, which is for electronic components' protection. The third part is the brackets, where there are four brackets to support the landing force. The brackets are locked between the frame and the carriage. The fourth part is the hook cover mechanism, which is used to close the upper side of the casing.

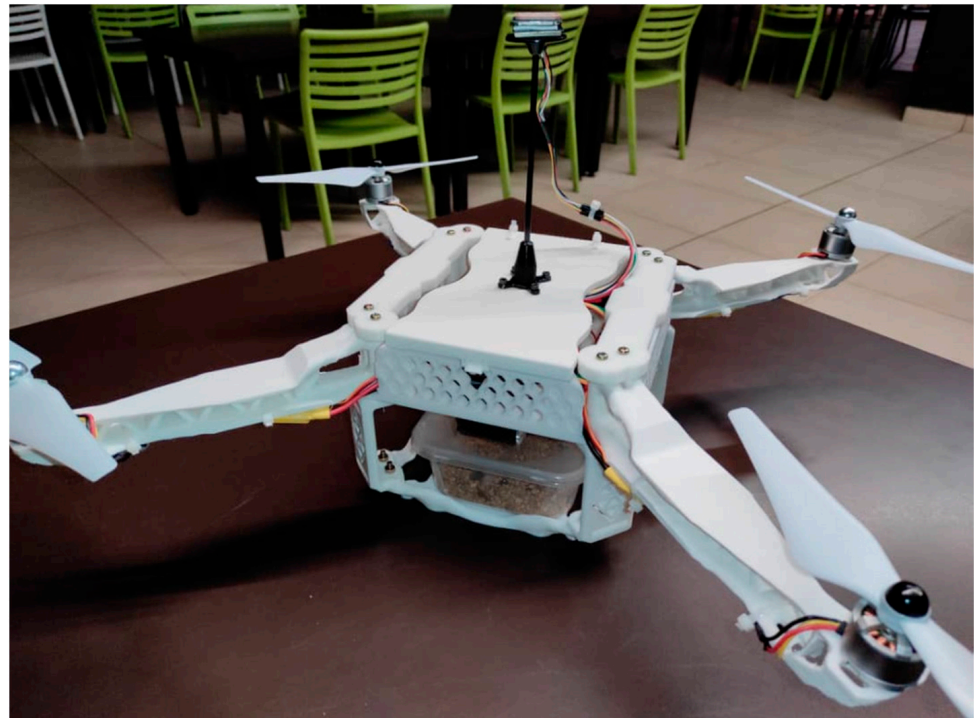


**Figure 17.** Hardware of the Drone Design.

#### 4.5. Three Dimensional Printing Process

The drone was printed using the ANYCUBIC I3 MEGA. The Cura software was used to convert stl file format into G-code format to print the drone parts. The infill was set to 100% to increase the design structure strength. The types of filament used were PLA; 195 degree Celsius is the standard to print PLA material. The retraction speed was adjusted to 40 mm/s. The retraction distance was adjusted to 4.5 mm, the layer height adjusted to 0.2 mm, and the bed temperature was set to 60 degree Celsius. It takes an average of 6 h to print a part. The steps listed below were followed:

1. Download and install Cura.
2. Slice the 3D model into smaller pieces.
3. Three Dimensional model saved to an SD card as G-Code.
4. SD card is inserted into the 3D printer.
5. Load filament into the 3D printer.
6. Activate the printing application.

#### 5. Conclusions

Modelling for a drone's parts has been presented in this project. Simulation of the parts was conducted using the 3DEXPERIENCE software, which provides modelling, simulation, and optimization functions, to obtain the best design option and to make sure that the final design of the parts was aesthetically novel with no un-smooth edges or uneven shapes. Simulation of the drone's stress and displacement was carried out, where the results show that the drone frame will not fail when it needs to sustain the maximum possible lift force from the motor as well as during the landing process. In addition, the concept shapes that were generated were compared by performing a trade-off study. The variants assessed were the mass, the displacement, and the stress of the parts. Simulation of the drone's weight was carried out for the center top cover (50 g), side top cover (10 g), middle cover (30 g), and drone's arm (80 g). The simulation of the parts was performed by using 3D Designer; hence, more details can be obtained through the trade-off study and the simulation of the drone's weight.

**Supplementary Materials:** The following supporting information can be downloaded at: <https://www.mdpi.com/article/10.3390/drones6040097/s1>, Figure S1: Dimension of drone Leg breaket; Figure S2: Dimension of drone side top cover. Figure S3: Dimension of drone arm, Figure S4: Dimension of drone midell cover, Figure S5: 3D printer model, Figure S6: Side top cover, meddle cover and center top cover of the drone, Figure S7: Description of 3D printed parts.

**Author Contributions:** Methodology, A.O.M. and H.C.; software, P.U.; validation, K.Y. and H.C.; formal analysis, T.J.; investigation, T.J.; writing—original draft preparation, A.O.M., H.C., P.U. and T.J.; writing—review and editing, A.O.M. and K.Y.; supervision, K.Y. and H.C.; funding acquisition, K.Y. and H.C. All authors have read and agreed to the published version of the manuscript.

**Funding:** This research was funded by [Sunway University postgraduate studentship and School of Engineering UOW Malaysia KDU Penang University College, Postgraduate & Research Centre (PGRC)]. And the APC was funded by [Sunway University postgraduate studentship and School of Engineering UOW Malaysia KDU Penang University College, Postgraduate & Research Centre (PGRC)].

**Institutional Review Board Statement:** Not applicable.

**Informed Consent Statement:** Not applicable.

**Acknowledgments:** We would like to acknowledge the support of Sunway University postgraduate studentship and School of Engineering UOW Malaysia KDU Penang University College, Postgraduate & Research Centre (PGRC). Additionally, we would like to acknowledge the help in 3D printing and fabrication by: Lee Wei Hou, Chan Lap Foong, Seerla Kanagarajoo, Betharajoo, and Simon Anandaraj Doss.

**Conflicts of Interest:** The authors declare no conflict of interest.

## References

- Oakey, A.; Waters, T.; Zhu, W.; Royall, P.; Cherrett, T.; Courtney, P.; Majoe, D.; Jele, N. Quantifying the Effects of Vibration on Medicines in Transit Caused by Fixed-Wing and Multi-Copter Drones. *Drones* **2021**, *5*, 22. [CrossRef]
- Hiebert, B.; Nouvet, E.; Jeyabalan, V.; Donelle, L. The Application of Drones in Healthcare and Health-Related Services in North America: A Scoping Review. *Drones* **2020**, *4*, 30. [CrossRef]
- Akhloufi, M.; Couturier, A.; Castro, N. Unmanned Aerial Vehicles for Wildland Fires: Sensing, Perception, Cooperation and Assistance. *Drones* **2021**, *5*, 15. [CrossRef]
- Barreto, J.; Cajaiba, L.; Teixeira, J.; Nascimento, L.; Giacomo, A.; Barcelos, N.; Fettermann, T.; Martins, A. Drone-Monitoring: Improving the Detectability of Threatened Marine Megafauna. *Drones* **2021**, *5*, 14. [CrossRef]
- A Game Changer for Business and Innovation. Available online: <https://www.3ds.com/3dexperience> (accessed on 28 February 2022).
- Royo, P.; Pastor, E.; Barrado, C.; Cuadrado, R.; Barrao, F.; Garcia, A. Hardware Design of a Small UAS Helicopter for Remote Sensing Operations. *Drones* **2017**, *1*, 3. [CrossRef]
- Dawkins, J.; Devries, L. Modeling, Trim Analysis, and Trajectory Control of a Micro-Quadrotor with Wings. *Drones* **2018**, *2*, 21. [CrossRef]
- Shukla, D.; Komerath, N. Multirotor Drone Aerodynamic Interaction Investigation. *Drones* **2018**, *2*, 43. [CrossRef]
- Castiblanco, J.M.; Garcia-Nieto, S.; Simarro, R.; Salcedo, J. Experimental study on the dynamic behaviour of drones designed for racing competitions. *Int. J. Micro Air Veh.* **2021**, *13*, 17568293211005757. [CrossRef]
- Basson, C.; Hansraj, S.; Stopforth, R.; Mooney, P.; Phillips, R.; Van Niekerk, T.; Du Preez, K. A Review of Collaborated Educational Drone Development and Design at the BRICS 2018 Future Skills Challenge. In Proceedings of the 2019 Southern African Universities Power Engineering Conference/Robotics and Mechatronics/Pattern Recognition Association of South Africa (SAUPEC/RobMech/PRASA), Bloemfontein, South Africa, 28–30 January 2019; pp. 17–22. [CrossRef]
- Jo, B.W.; Song, C.S. Thermoplastics and Photopolymer Desktop 3D Printing System Selection Criteria Based on Technical Specifications and Performances for Instructional Applications. *Technologies* **2021**, *9*, 91. [CrossRef]
- Horvath, J.; Cameron, R. The Desktop 3D Printer. In *3D Print with MatterControl*; Springer: Berkeley, CA, USA, 2015; pp. 3–13. [CrossRef]
- Kacmarcik, J.; Spahic, D.; Varda, K.; Porca, E.; Zaimovic-Uzunovic, N. An investigation of geometrical accuracy of desktop 3D printers using CMM. *IOP Conf. Series: Mater. Sci. Eng.* **2018**, *393*, 012085. [CrossRef]
- 3D Printing Third Edition. Available online: <https://lib.hpu.edu.vn/handle/123456789/31244> (accessed on 27 February 2022).
- Shahrubudin, N.; Lee, T.; Ramlan, R. An Overview on 3D Printing Technology: Technological, Materials, and Applications. *Procedia Manuf.* **2019**, *35*, 1286–1296. [CrossRef]
- Arefin, A.; Khatri, N.; Kulkarni, N.; Egan, P. Polymer 3D Printing Review: Materials, Process, and Design Strategies for Medical Applications. *Polymers* **2021**, *13*, 1499. [CrossRef]

17. Antreas, K.; Piromalis, D. Employing a Low-Cost Desktop 3D Printer: Challenges, and How to Overcome Them by Tuning Key Process Parameters. *Int. J. Mech. Appl.* **2021**, *10*, 11–19. [[CrossRef](#)]
18. Haryńska, A.; Carayon, I.; Kosmela, P.; Szeliski, K.; Łapiński, M.; Pokrywczyńska, M.; Kucińska-Lipka, J.; Janik, H. A comprehensive evaluation of flexible FDM/FFF 3D printing filament as a potential material in medical application. *Eur. Polym. J.* **2020**, *138*, 109958. [[CrossRef](#)]
19. Krishnanand; Soni, S.; Taufik, M. Design and assembly of fused filament fabrication (FFF) 3D printers. *Mater. Today Proc.* **2020**, *46*, 5233–5241. [[CrossRef](#)]
20. Vasudevarao, B.; Natarajan, D.P.; Henderson, M. Sensitivity of Rp Surface Finish to Process. In Proceedings of the 2000 International Solid Freeform Fabrication Symposium, Austin, TX, USA, 25–27 July 2000; pp. 251–258.
21. Galatas, A.; Hassanin, H.; Zweiri, Y.; Seneviratne, L. Additive Manufactured Sandwich Composite/ABS Parts for Unmanned Aerial Vehicle Applications. *Polymers* **2018**, *10*, 1262. [[CrossRef](#)]
22. Bishay, P.L.; Burg, E.; Akinwunmi, A.; Phan, R.; Sepulveda, K. Development of a New Span-Morphing Wing Core Design. *Designs* **2019**, *3*, 12. [[CrossRef](#)]
23. Sharma, V. Advances in Drone Communications, State-of-the-Art and Architectures. *Drones* **2019**, *3*, 21. [[CrossRef](#)]
24. Muralidharan, N.; Pratheep, V.; Shanmugam, A.; Hariram, A.; Dinesh, P.; Visnu, B. Structural analysis of mini drone developed using 3D printing technique. *Mater. Today Proc.* **2021**, *46*, 8748–8752. [[CrossRef](#)]
25. Negrelli, V. “From earth to heaven”: How professional 3D Printing and Windform® GT material helped in the construction of drone and medical devices. *Reinf. Plast.* **2017**, *61*, 179–183. [[CrossRef](#)]
26. Kantaros, A.; Diegel, O. 3D printing technology in musical instrument research: Reviewing the potential. *Rapid Prototyp. J.* **2018**, *24*, 1511–1523. [[CrossRef](#)]
27. Shen, C.H.; Albert, F.Y.C.; Ang, C.K.; Teck, D.J.; Chan, K.P. Theoretical development and study of takeoff constraint thrust equation for a drone. In Proceedings of the 2017 IEEE 15th Student Conference on Research and Development (SCoReD), Wilayah Persekutuan Putrajaya, Malaysia, 13–14 December 2017; pp. 18–22. [[CrossRef](#)]
28. Research and Development in Modern Materials. Available online: <https://blogs.deakin.edu.au/remstep/materials-activities/honeycomb-structures/> (accessed on 1 January 2022).
29. Amza, C.G.; Zapciu, A.; Eypórsdóttir, A.; Björnsdóttir, A.; Borg, J. Mechanical properties of 3D printed composites with ABS/ASA substrate and glass fiber inserts. In Proceedings of the MATEC Web of Conferences, Kursk, Russia, 1 November 2019; Volume 290, p. 04002. [[CrossRef](#)]
30. Afshar, A.; Wood, R. Development of Weather-Resistant 3D Printed Structures by Multi-Material Additive Manufacturing. *J. Compos. Sci.* **2020**, *4*, 94. [[CrossRef](#)]
31. Butt, J.; Bhaskar, R. Investigating the effects of annealing on the mechanical properties of FFF-printed thermoplastics. *J. Manuf. Mater. Process.* **2020**, *4*, 94. [[CrossRef](#)]
32. Comparing 3D Printing Filament Features: ABS vs. ASA Filament. Available online: <https://www.makeshap-er.com/2020/01/24/3d-printing-filament-features-abs-vs-asa-filament/> (accessed on 28 February 2022).
33. Iannace, S.; Sorrentino, L.; Di Maio, E. *Biodegradable Biomedical Foam Scaffolds*; Woodhead Publishing Limited: Federico II, Italy, 2014; pp. 163–187. [[CrossRef](#)]
34. Malaysian Information Climate. Available online: <https://www.malaysia.gov.my/portal/content/144> (accessed on 28 February 2022).
35. Rayna, T.; Striukova, L. From rapid prototyping to home fabrication: How 3D printing is changing business model innovation. *Technol. Forecast. Soc. Chang.* **2016**, *102*, 214–224. [[CrossRef](#)]
36. Brischetto, S.; Torre, R. Preliminary Finite Element Analysis and Flight Simulations of a Modular Drone Built through Fused Filament Fabrication. *J. Compos. Sci.* **2021**, *5*, 293. [[CrossRef](#)]
37. Kantaros, A.; Piromalis, D.; Tsaramirsis, G.; Papageorgas, P.; Tamimi, H. 3D Printing and Implementation of Digital Twins: Current Trends and Limitations. *Appl. Syst. Innov.* **2022**, *5*, 7. [[CrossRef](#)]
38. Kantaros, A.; Karalekas, D. FBG Based In Situ Characterization of Residual Strains in FDM Process. *Conf. Proc. Soc. Exp. Mech. Ser.* **2014**, *8*, 333–337. [[CrossRef](#)]
39. 3D Robotics IRIS + RTF Kit (433). Available online: <https://www.megapixel.cz/3d-robotics-iris-433> (accessed on 2 March 2022).
40. Skeleton X-14 Quadcopter. Available online: <https://cults3d.com/en/3d-model/gadget/skeleton-x-14-quadcopter> (accessed on 2 March 2022).